Nonlin. Processes Geophys. Discuss., 2, 69–96, 2015
www.nonlin-processes-geophys-discuss.net/2/69/2015/
doi:10.5194/npgd-2-69-2015

Nonlinear Processes in Geophysics
Discussions
Open Access

Non-local deformation effects in shear flows

A. V. Popova[1,2], O. V. Sheremetyeva[1,2], M. E. Bobrova[1], and A. S. Perezhogin[1]

[1]Institute of Cosmophysical Researches and Radio Wave Propagation FEB RAS, Kamchatskiy Kray, Paratunka, Russia
[2]Vitus Bering Kamchatka State University, Petropavlovsk-Kamchatskiy, Russia

Received: 28 October 2014 – Accepted: 23 December 2014 – Published: 21 January 2015

Correspondence to: A. V. Popova (non-ame@li.ru)

Published by Copernicus Publications on behalf of the European Geosciences Union & the American Geophysical Union.

Abstract

The method for detection of clusters on the basis of event space–time dependence is classically applied for foreshock–mainshock–aftershock sequences for which event connectedness is generally accepted. In the paper, this approach is used to investigate the whole event catalogue of foreshock and aftershock sequences filtered from the events with small magnitudes, in which connected events are also determined. The space scale is extended due to the inclusion of the parameter of seismic event connectedness in the direction of dislocation shift that allows us to consider the obtained connected events as clusters in a shear flow. A statistical model of the shear flow was constructed by catalogue decomposition into timescales and space scales defined analytically. A modelling algorithm of the shear flow was developed and its stability to initial condition change was investigated. Shear flow structure and arising non-local deformation characteristics which may be the criteria for dynamic process activity in the considered subduction zone of the Kuril–Kamchatka island arc were analysed.

1 Introduction

From the point of view of the specialists of the earth sciences, seismic events with the given energy concentrated in some volume form a Poisson flow of independent events, and the waiting periods for the next event are distributed according to the exponential law and are independent, but at the present stage of modelling of a seismic process, the known spatial and time laws (Gutenberg–Richter law, Omori law, Kaiser effect, etc.) are widely used, which allows us to determine the dependences between seismic events (Kagan and Knopoff, 1977; Lukk et al., 1996; Shebalin, 2006; Shevtsov and Sagitova, 2009). This means that description of the seismic process as a usual Poisson one is not always satisfactory (Goldin, 2004; Vinogradov and Ponomarev, 1999; Sobolev, 2003), and scientists build new models (Kagan and Knopoff, 1977; Shebalin, 2006; Shevtsov and Sagitova, 2009, 2012) where the cause–effect relation between seismic

NPGD
2, 69–96, 2015

events is detected and non-local properties in time and space in the catalogue are under investigation.

The method of estimation of the space–time connectedness of seismic events is widely used to investigate aftershock–mainshock–foreshock sequences, and the space and time connectedness criteria are introduced as analytical ones on the basis of known laws and determined statistically (Shebalin, 2006; Shevtsov and Sagitova, 2009, 2012; Kagan and Knopoff, 1977; Anderson and Nanjo, 2013; Batac and Kantz, 2014; Zaliapin and Ben-Zion, 2013; Zaliapin et al., 2008; Saichev and Zaslavsky, 1997; Saichev and Sornette, 2006; Sornette and Helmstetter, 2002). Extensive investigations into this issue were carried out by Kagan and Knopoff (Kagan and Knopoff, 1977, 1980, 1981), in which, on the basis of the stochastic approach, the authors determined both time and space parameters of the connectedness as well as the limits of their application due to seismicity chaotic properties which appeared as a non-linear dynamic fracture process in elastic oscillations. Comparative analysis of model constructions and experimental data on the detection of the location of a next seismic event in a sequence was also performed.

Another class of paper in this direction is devoted to the study of the conditions for deviation of seismicity from normal regimes (Shebalin, 2006; Sornette and Helmstetter, 2002). According to the ideas of critical phenomenon theory, seismicity deviations from the normal behaviour are called sub- and super-critical regimes of earthquakes. Within the framework of the plasticity theory, it is associated with the amplification of viscous and fragile processes, and from the point of view of the statistical theory, it is the effect of anomalous delays and remote space correlations (Sornette and Helmstetter, 2002). In a dislocation group, in the conditions close to critical ones, collective phenomena with memory or non-localness may occur, and in statistical distribution, degree regimes showing the complicated space–time self-organisation of the seismicity appear (Saichev and Sornette, 2006). Depending on the prevailing regime, the character of the process changes.

The recent papers continue the investigations of characteristic peculiarities in the behaviour of statistical distributions of seismic event space–time separation for global and regional seismicity (Zaliapin et al., 2008) as well as the search for the simplest and most reliable criteria for separating connected and unconnected events in full catalogues that are the characteristics of laws in the statistical distributions (Anderson and Nanjo, 2013; Batac and Kantz, 2014). In the present paper, the methods for timescale and space scale decomposition of foreshock and aftershock catalogues, filtered from events with small magnitudes, investigate the structure of the shear flow in the region and its deformation characteristics. The research is based on the stochastic model of a seismic process which is considered a Poisson complicated process and is decomposed into energy components. In that case, the possibility of occurrence of the next event with the given energy will depend only on time $P_i(t)$. Further space distribution of events may be defined for each component that enlarges the range of parameters in the formula for calculation of the probability of the next event. The obtained process of this approach is the composition of embedded processes where the probability of occurrence of an event with number i is a function of spatial–temporal parameters and energies of the preceding events $P_i(t, \boldsymbol{r}, \boldsymbol{u}, E)$, where t is the time, $\boldsymbol{r}$ is the radius vector from the initiating event to the related one, $\boldsymbol{u}$ is the shear direction and E is the energy of the event. The generalisation of such kinds of discrete random processes is the process of random walks (Shevtsov and Sagitova, 2009, 2012), which may be compared with the generalised diffusion process (Metzler and Klafter, 2000; Saichev and Zaslavsky, 1997). This approach is determined by the fact that seismic phenomena may be considered weak fluctuations, since, as a rule, the spatial scale of the region, where a geodynamic process develops, significantly exceeds the size of the earthquake focus and the radius of the area of influence where stress drops (i.e. the criterion of increment infinitesimality, if fulfilled).

According to the theoretical assumptions of the excepted phenomenological model, the paper investigates the earthquake catalogue for the possibility of detection of related events. The criterion for a pair relation of events is defined according to the notion

NPGD
2, 69–96, 2015

of the area of influence of a seismic event. The conception of scales, on which a pair of events is considered to be related, is introduced: firstly, the complicated Poisson process is decomposed into components according to event energies that determine the energy scale; secondly, it is possible to define the pairwise relation of seismic evens for each component of the Poisson process using the well-known Gutenberg–Richter law, which determines the timescale; and, thirdly, it is possible to define the pairwise relation of events for every component by introducing the spatial scale on the basis of a linear theory of elasticity. It is known that a system of cracks is formed around the earthquake focus. It is an area of partial failure with pronounced fractal properties. This zone is manifold larger than the focus and far less than the area of influence which is determined by elastic local deformations formed in the result of the failure. The scale of the event influence zone in space depends on the energy of this event and may be calculated by one of the techniques (Shevtsov and Sagitova, 2009, 2012; Shebalin, 2006; Dobrovolskiy et al., 1979; Perezhogin et al., 2007), as threshold values dividing the events connected with an initiating event from unconnected ones are the radii of event effects and space and time ones. The radius of space event connectedness is introduced analytically on the basis of two modes, Dobrovolskiy and Mindlin models. Comparative analysis of the results of model application for determination of the threshold value of a seismic event effect radius is carried out. The radius of time connectedness is also introduced analytically via the Gutenberg–Richter law. These two parameters have the information on the event magnitude and energy. In this study, the number of parameters was extended due to the statistically determined parameter for dislocation shift directions. Introduction of a new parameter allows us to consider the forming connected events as clusters in the shear flow in the region. Such an approach will help to determine the flow structure and to calculate fundamental deformation characteristics determining the degree of deformation process activity in the region.

In the paper (Shebalin, 2006), the relationship between the events is determined according to the size of the partial failure area, which corresponds to the fault zone or a system of foreshocks and aftershocks together with the principal shock, and by

NPGD
2, 69–96, 2015

the proximity of the events falling within the time interval which does not exceed the timescale determined by the event energies in linear constructions. Thus, the events are almost simultaneous and the spatial correlation radius is estimated by the number of events in linear constructions, and goes to infinity in critical conditions. This criterion for the space relation of events is stricter than that in the paper (Shevtsov and Sagitova, 2009), where the zone of influence defined by elastic local deformations was applied. In the papers (Shevtsov and Sagitova, 2009, 2012), criteria for a pair relation of events on the given spatial–temporal scales were determined and the full seismic catalogue was decomposed into a set of sequences; each of them was a Markov-type process, which, in fact, distinguishes this investigation from the paper (Shebalin, 2006).

The approach applied in the paper for the investigation of the catalogue develops the ideas of the article (Shevtsov and Sagitova, 2009), but in contrast to that research (Shevtsov and Sagitova, 2009; Anderson and Nanjo, 2013; Batac and Kantz, 2014), the spatial scale includes several characteristics. In particular, besides the spatial radius of the area of influence, new characteristics were introduced, such as fracture plane orientation and shear direction (Aki and Richards, 1983; Kostrov, 1975; Riznichenko, 1965). If spatial scales and timescales are considered, then a pair of events falling within the area limited by these scales may be considered to be related. This pair forms the simplest non-locality, the pair one. If such pairs form chains from three and more events, it indicates the relation of events in the catalogue, the dependence of increments and the occurrence of non-local deformation effects (Kagan and Knopoff, 1977; Shebalin, 2006; Shevtsov and Sagitova, 2009, 2012).

Thus, the present investigation suggests that an earthquake in the catalogue may be represented as a flow of pairwise related random events, the cluster length of which may be interpreted as a measure of non-locality in a Markov sequence. If only a timescale was used in the construction of a cluster, simple Markov chains with independent increments are formed. If the spatial scale is also applied, non-locality may arise in the cluster that means increment dependence. When the number of the cluster links goes to infinity, the process is a fundamentally non-Markov one, but it is impossible to ascertain the latter due to the limited statistics. However, there is a possibility of investigating the catalogue on the basis of the given phenomenological model of the seismic process to determine the shear flow cluster structure (of the whole catalogue). The novelty of the approach is the extension of probability parameters that allows one to represent the seismic process as a flow of random events with the defined direction of dislocations and to consider it as a dislocation flow in the region, the markers of which are the seismic events joined into clusters; moreover, the clusterisation method is applied to the whole catalogue filtered from foreshocks and aftershocks. Furthermore, the determined clusters are used to study the parameters of stress and strain media states in the seismically active region and to detect such fundamental properties of the seismic process as flow direction and velocity which characterise the orientation and the velocity of seismogeodynamic processes in the region (Gordeev et al., 2001; Kostrov, 1975; Lomize, 1999; Rebetskii, 2007; Riznichenko, 1965).

Thus, two tasks are solved in the paper: firstly, applying the stochastic description of the seismic process, to determine the event effect radius values, to develop the criteria of event connectedness and the algorithm of construction of shear flows; secondly, according to the data of the filtered catalogue, to construct a stochastic model of the shear flow in the region, to analyse both non-local effects occurring there and the parameters of the medium stress–strain state. When choosing the real catalogue for the investigation, the major requirement was the presence of the parameters determining the direction and the magnitude of a shear along a dislocation (Aki and Richards, 1983). Only the Global CMT catalogue (Global CMT Web Page, 2010) fully met these criteria. Such a model for the subduction zone of the Kuril–Kamchatka island arc has been constructed for the first time.

2 Modelling algorithm for the shear flow

Non-local effects of the seismic process appear as a cluster covering long time intervals and spatial domains (Kagan and Knopoff, 1977; Shebalin, 2006; Shevtsov and

NPGD
2, 69–96, 2015

Sagitova, 2009). Extension of the criteria for event connectedness due to the introduction of a dislocation shift direction allows us to consider the seismic process as a flow of random events with the defined shear direction, and the formed sequences may be interpreted as clusters in the shear flow. Note that cluster formation should not be considered a manifestation of local effects. Determination of clusters indicates only the possible connection of the events as a result of deformation disturbances. A non-localness feature is the anomalous, super- or sub-diffusion character of random walks in the clusters.

The spatial–temporal scales of decomposition of the seismic event catalogue are defined by media characteristics and the seismic process. The parameters for the area of influence of the initiating seismic event are defined as follows:

1. *Timescale* t (days) is estimated on the basis of the Gutenberg–Richter recurrence law for each seismic event as the relation

$$R_t = \frac{T}{n}, \tag{1}$$

where T is the time period of the catalogue expressed in days, n is the number of events with M_L magnitude (the chosen sampling interval $\Delta = 0.1$), M_L is the Richter magnitude, which is calculated by the following formula (Hanks and Boore, 1984),

$$M_L = \frac{\lg M_0 - 17.0}{1.4}, \tag{2}$$

and M_0 $(N \cdot m)$ is a seismic moment (Global CMT Web Page, 2010).

2. The *spatial scale* is determined by two parameters:

   – *Radius* R_d (km) *of the area of influence* of a seismic event on the basis of two models:

NPGD
2, 69–96, 2015

a. the Dobrovolskiy model (Dobrovolskiy et al., 1979)

$$R_d = 10^{0.43 M_L}, \quad (3)$$

b. and the Mindlin model with the combination of double forces determined by seismic moment tensor values. The value of the maximal shear deformation 10^{-8} is used as an evaluative parameter to calculate the distance; i.e. the radius is determined from the focus centre to the terminal point, with the level of tidal deformations of 10^{-8} (Perezhogin et al., 2007).

– Shear vector *scattering angle* MAD:

$$\mathrm{MAD} = \arctan\sqrt{\frac{\lambda_{\min} + \lambda_{\max}}{\lambda_{\mathrm{int}}}}, \quad (4)$$

where λ are the eigenvalues of the covariance matrix of the shear single vector sampling (Davis, 1986; Mardia, 1972). Statistical analysis of the catalogue data for the considered sampling gave a deflection angle value of 24°.

Construction of the sequence of related seismic events, forming a cluster in a shear flow, is determined by the closeness of events in the future relative to the initiating event on the basis of the input threshold and criteria. In the developed algorithm, the block diagram of which is shown in Fig. 1, the events with *j* numbers will fall within the area of influence of the earlier (initiating) seismic event, the number of which in the sampling is *i*. These events meet the following criteria:

1. The time interval between the considered and initiating events does not exceed the timescale R_t of the initiating event:

   $$\Delta t = (t_j - t_i) \le R_t.$$

2. Spatial parameters of the considered pair of seismic events do not exceed the spatial scale of the initiating event:

NPGD
2, 69–96, 2015

– the distance between the hypocentres of the considered pair of seismic events does not exceed the spatial radius R_d of the area of influence of the initiating event:

$$\Delta d = |\mathbf{r}_j - \mathbf{r}_i| \leq R_d;$$

– angles of shear direction deflection of the considered pair of seismic events do not exceed the scattering angle MAD = 24° for the sampling under consideration.

3. Among the set of events falling within the spatial–temporal region with regard to the shear direction, an event with a comparable energy (or magnitude M_{max}) is chosen.

Investigation of the problem of the algorithm stability to the change in initial conditions was carried out as follows: data pieces of different lengths were removed from the beginning of the pilot sample and the developed algorithm was applied to the obtained sample. The results showed that the general structure of the flow did not change significantly. As a rule, in three or four steps, the nodal state is achieved in the sequence of related events, after which the walks repeat their ways in the cluster obtained from the initial sample which indicated the stability of the suggested algorithm to initial condition change. Thus, it is possible to begin building clusters from any event in the catalogue.

3 Statistical model of the shear flow

The described algorithm allows us to build a statistical model of the shear flow in a seismically active region and to analyse non-local deformation effects of the flow under consideration of its basis. 221 events were used from the CMT catalogue (Global CMT Web Page, 2010) to study the subduction zone of the Kuril–Kamchatka island

NPGD
2, 69–96, 2015

arc. They occurred within the period of 1976–2005 with the depth range of 10–60 km (magnitudes are 4.5–7.7, and the area is 50–60° N, 156–166° E). The choice of the depth range is explained by the difference in earthquake mechanisms occurring deeper (Riznichenko, 1965), and the distribution of seismic events in this range may be considered uniform.

Applying the developed algorithm, the sample from the CMT catalogue (Global CMT Web Page, 2010) was decomposed into non-overlapping sequences of related events on the basis of introduced criteria. The related events form a sequence according to the increase in their numbers in the sample. Each of these sequences containing not less than three events is interpreted as a cluster in the shear flow, the flow direction in which is determined by the direction of shears of included events, and the continuity of the seismic process is provided by the intersection of the areas of their influence. Numbering of every cluster in the shear flow is according to the first event included.

The fraction of the events, joined into clusters, if the threshold value for space radius was calculated according to the Dobrovolskiy model, turned out to be 0.6 (Table 1), and according to the Mindlin model, it is 0.3 (Table 2). Note that the threshold values of the event effect radius in space determined according to the Mindlin model have the same order as those obtained in the paper (Anderson and Nanjo, 2013; Batac and Kantz, 2014). The correlation coefficient for the applied spatial radii is close to the unit due to the general theoretical foundations of both models, but the Mindlin spatial radius values are 3.5 times less than the Dobrovolskiy radius. This results in the narrowing of the area of influence of the event in space and, as a consequence, in the decrease in the related event number. The non-overlapping clusters whose spatial scale is determined by the spatial radius of the Dobrovolskiy model are related and form a single structure of the shear flow in the region. Application in the calculation of the spatial radius of the Mindlin model entails the decrease in the number of events forming a cluster and the increase in the number of independent clusters that are the parts of the clusters, obtained by the Dobrovolskiy spatial radius. Nevertheless, irrespective of the model of calculation, sequences of related events, i.e. clusters, where walks

NPGD
2, 69–96, 2015

are realised unevenly, are formed, which indicates the presence of non-local spatial–temporal effects.

The most extensive clusters and the parameters of included seismic events are illustrated in Tables 1 and 2 and, correspondingly, in Figs. 2 and 3, where the biggest faults (1) and deep-sea trench axes (2), Kuril–Kamchatka (K–K) and Aleutian (A), are illustrated schematically, black arrows indicate the projections of dislocation shear direction, the bold black arrow is the projection of the main flow direction in a cluster, and the blue arrow consequently joins the related events.

Analysis of the statistical model for the shear flow indicates that application of the Dobrovolskiy model and the Mindlin model allows us to obtain clusters covering extensive time intervals and spatial domains. Inside the clusters, the tramping in a limited area is changed by long spans (Fig. 2), i.e. short- and long-range correlation effects are realised which appear as non-local properties of walks. Irregularity of walks is associated with medium property change and stress that must affect the deformation properties, in particular, in relative deformation rates, allowing us to determine the degree of deformation process activity. Though the stochastic approach does not allow us to make forecasts of the direction and the rate of seismic process development, there are some regularities. For example, slowing down of the relative deformation rate in clusters may be considered an accumulation of seismic energy in space regions in which the process activity decreased as the result of medium hardening and increase in elastic energy that inevitably lead to failures ("seismic break" by Fedotov, Kaizer effect), since preparation of failures appears as the effect of remote correlations between the events (Shebalin, 2006). The obtained results agree well with the results of the paper (Shevtsov and Sagitova, 2012) for the same region based on the earthquake catalogue of the Kamchatka branch of the Geophysical Service of the Russian Academy of Sciences for the period from 1 January 1962 to 31 December 2002 without limitations for the event parameters with the energy not less than the ninth class.

NPGD
2, 69–96, 2015

4 Shear flow characteristics

Characteristics of the shear flow in the region are investigated on the basis of the developed statistical model. The following parameters were determined for the obtained clusters: the number of included events k, the time period of the cluster τ (years), summary ΣE and average $\overline{E}$ energy, average shear $\overline{u}$ (sm), the angle γ between the projection on the Earth surface plane of the shear main direction in the cluster and the direction to the north in the local coordinate system, mean square deviation (MAD), the flow average velocity $\overline{v}$ in the cluster, and the relative deformation rate ξ.

The summary energy ΣE determining the stress and strain state in the cluster was calculated from the seismic energy of the included events:

$$\Sigma E = \sum_{i=1}^{k} E_i, \tag{5}$$

where E_i is the energy of the event in the cluster

$$E_i = 10^{1.5M_\mathrm{L}+4.8}. \tag{6}$$

Average shear $\overline{u}$ is equal to the relation of the summary shear to the number of events k in the cluster

$$\overline{u} = \left(\sum_{i=1}^{k} u_i\right)/k, \tag{7}$$

where the shear value u_i for each event falling within the cluster was determined on the basis of the known scalar seismic moment M_0 (Global CMT Web Page, 2010), basalt shear modulus $\mu \approx 3.14 \times 10^{10}$ (Nm^{-2}) (Kozlovskii, 1984) and fracture size S (Gusev and Melnikova, 1990) from the relation (Aki and Richards, 1983)

$$u_i = \frac{M_{0i}}{\mu \cdot S_i}. \tag{8}$$

NPGD
2, 69–96, 2015

Non-local deformation effects in shear flows

A. V. Popova et al.

The average velocity of the flow in the cluster was estimated as the relation of the sum of dislocation shears in some volume to time period τ of the cluster lifetime in the shear flow (Aki and Richards, 1983; Kozlovskii, 1984; Riznichenko, 1965)

$$\overline{v} = \left(\sum_{i=1}^{k} u_i\right) / \tau. \tag{9}$$

The average velocity of lithospheric plate movement on the surface of the Kuril–Kamchatka island arc subduction zone, measured according to GPS observation data, is 8 sm year^{-1} (Gordeev et al., 2001; Lomize, 1999). The relative deformation rate ξ of the considered shear flow was calculated as the following relation:

$$\xi = \frac{(\overline{v} - 8)}{h_{\max}}. \tag{10}$$

As was noted above, relative deformation rate change in clusters of the shear flow may indicate the increase or slowing down of the deformation process in the region. Tracing of such characteristics may allow us to make diagnostics of changes in deformation process activity, in particular, the intensification or slowing down in the region covered by the cluster.

Average characteristics are calculated for the largest clusters in the shear flow and are shown in Tables 3 and 4. Among the clusters, obtained by the spatial radius of the Dobrovolskiy model (Table 3), the prevailing cluster no. 23 has the highest summary energy. This cluster is determined by ten events (Table 1), covering the time interval of 22.7 years and all the areas under consideration (Fig. 2). Cluster no. 47 is its substructure; it covers almost the same temporal–spatial domain, but has less summary energy. Cluster nos. 62, 77, 90, and 131 are the substructures of cluster no. 47 with less energies.

In the prevailing cluster, covering the largest part of the catalogue, the average rate of relative deformations is comparable with tides that are, generally, characteristic of

NPGD
2, 69–96, 2015

extensive time and space clusters (Table 3) and that, most likely, determine the common tendency of the shear flow in the region. Nevertheless, in the dynamics of the deformation rate changes in a cluster, irregularity is observed, periods of increase are changed by periods of decrease that are an indication of deformation process regime change associated either with medium hardening and the increase in elastic energy, or with stress drop accompanied by failure. Shorter clusters forming a substructure of the prevailing one have average values of relative deformation rates which are 1 order and higher than tidal ones, which is explained by their narrower space–time location and gives information on the deformation process in the region limited by the cluster.

Clusters, obtained by the spatial radius calculated according to the Mindlin model (Table 4), include fewer events. The prevailing cluster was not determined as long as the general structure which had been obtained earlier fell into the clusters which characterise the specific character of the shear flow in the region limited by every cluster. Cluster no. 46 has the highest summary energy. It is determined by six events (Table 2), and covers the time period of 18.2 years (Fig. 3) and relative deformation rate which is equal in order to the tidal one. Among the clusters in Table 4, only cluster nos. 111 and 112 are related. Average values of relative deformation in clusters exceed the tidal ones by several orders.

5 Discussion and conclusions

Non-local deformation effects in the seismic process appear as the anomalous character of the random walk in the clusters of the shear flow. To carry out such an investigation of the real catalogue, the paper defines the scales and criteria for seismic event relations; they are spatial, temporal and energy ones. Extension of the space criteria due to the introduction of the spatial criteria of such a parameter as dislocation shear direction gave the possibility of considering the seismic process as a shear flow in the region and developing the modelling algorithm for the brittle component of plastic deformation, i.e. shear flows.

The authors determined the stability of the algorithm to initial condition change that allows them to begin statistical modelling from any event in the catalogue. Applying the developed algorithm, the statistical model of the shear flow of the Kuril–Kamchatka island arc subduction zone was built for the first time on the basis of the Global CMT catalogue (Global CMT Web Page, 2010) with a depth limitation of 10–60 km. Using the model, shear flow structure and deformation characteristics in the region were investigated.

The relation of the number of related events to the sample size determines the relation characteristic of the sample in temporal–spatial scales, taking into account event energies and dislocation shear directions. Applying the Dobrovolskiy model to calculate the threshold spatial radius of event influence, the relation characteristic is 0.6 and the generated clusters form a single structure of the shear flow, whereas for the Mindlin model, it is 0.3; lengths of the formed clusters decrease and the general structure falls into independent clusters. Spatial radii calculated on the basis of these two models are well correlated, but narrowing of the spatial area of influence of the event reduced the relation characteristic. It should be noted that the calculated main directions of the flows in the clusters have a north-western orientation, which agrees with the available geophysical data (Gordeev et al., 2001; Lomize, 1999). Angle distributions of dislocation shears in every cluster are spread relative to the main north-western direction within 9 to 18°. It indicated a good orientation of the shear flow.

Analysis of the statistical model of the shear flow showed that application of both the Dobrovolskiy and Mindlin models results in the formation of clusters covering extensive time intervals and spaces, where walks are realised irregularly, which agrees with the conclusions of the paper (Mardia, 1972). Close and remote correlation effects are associated with the change in medium properties and stress which one may judge by relative deformation rates. The order of relative deformation ξ rates in the longest clusters in the shear flow corresponds to tidal ones of 10^{-6} year^{-1}, and in shorter clusters it increases to 10^{-3} year^{-1}. This agrees with the conclusions of the research (Marapulets et al., 2012). The prevailing cluster in the shear flow was determined; its deformation

NPGD
2, 69–96, 2015

characteristics reflect general tendencies of the shear flow, whereas less extensive clusters, which are its substructures, determine the specific character of the deformation process in the local region, limited by the cluster.

The results of statistical modelling of the seismic process allow the authors to draw the conclusion on the relatedness of seismic events in the whole catalogue filtered by the foreshocks and the aftershocks and give the possibility of considering the mathematical models of the process filling it with non-locality and memory. For example, the model of the fractional Poisson process with order of differentiation $\alpha \in [0, 2]$ may be used. If the parameter α equals 2, the Poisson process obtained, for example, in the paper (Anderson and Nanjo, 2013) indicates that the declustered catalogues are much closer to Poissonian distribution than the originals. If the parameter $1 \leq \alpha \leq 2$, the tendency to "jumps" appears in the process (a super-diffusion process that corresponds to long time delays and distance increase between the vents in space, i.e. long-range spatial correlations). Probably, approximation to critical condition changes the character of the seismic process and determines the transfer from the Poisson law to other laws between the events that increases the relation of seismic events in the earthquake catalogue (the characteristic of catalogue relation). The investigation results may be applied further for the development of a method for evaluation of seismic risk in the region.

Acknowledgements. We thank B. M. Shevtsov for valuable advice, discussions and help in formulating some of our results, I. Zaliapin for the informative notes, as well as all who helped in preparing this manuscript for publication.

References

Aki, K. and Richards, P.: Quantitative Seismology, Theory and Methods, V.1, Mir, Moscow, 519 pp., 1983. 74, 75, 81, 82

Anderson, J. G. and Nanjo, K.: Distribution of earthquake cluster sizes in the Western United States and in Japan, B. Seismol. Soc. Am., 103, 412–423, 2013. 71, 72, 74, 79, 85

Batac, R. C. and Kantz, H.: Observing spatio-temporal clustering and separation using interevent distributions of regional earthquakes, Nonlin. Processes Geophys., 21, 735–744, doi:10.5194/npg-21-735-2014, 2014. 71, 72, 74, 79

Davis, J. C.: Statistics and data analysis in geology, 2nd edn., Kansas geological survey, John Wiley and Sons, New York, Chichester, Brisbane, Toronto, Singapore, 267 pp., 1986. 77

Dobrovolskiy, I. R., Zubkov, S. I., and Myachkin, V. I.: Estimation of the size of earthquake preparation zones, PAGEOPH., 117, 1025–1044, 1979. 73, 77

Global CMT Web Page, available at: http://www.globalcmt.org/, last access: 16 December 2010. 75, 76, 78, 79, 81, 84

Goldin S. V.: Dilatansiya, repacking and earthquakes, Phys. Earth, 10, 37–54, 2004. 70

Gordeev, E. I., Levin, V. E., Bakhtiyarov, V. F., Gusev, A. A., Pavlov, V. M., Chebrov, V. N., and Kasakhara, M.: Preliminary analysis of GPS station movements in Kamchatka: plate rate and earthquake geodesic precursor, geodynamics and vulcanizm of Krill-Kamchatka island-arc system, IVGG FEB RAS, Petropavlovsk-Kamchatsky, 82–94, 2001. 75, 82, 84

Gusev, A. A. and Melnikova, V. N.: Relations between magnitudes – global average and for Kamchatka, Vulkanology and seismology, V.6, Akademizdatcenter “Nauka” RAN, Moscow, 55–62, 1990. 81

Hanks, T. C. and Boore, D. M.: Moment-magnitude relations in theory and practice, J. Geophys. Res., 89, 6229–6235, 1984. 76

Kagan, Y. Y.: Likelihood analysis of earthquake catalogues, Geophys. J. Int. 106, 135–148, 1991.

Kagan, Y. Y.: Seismic moment distribution revisited, vol. I, statistical results, Geophys. J. Int., 148, 520–541, 2002.

Kagan, Y. Y.: Accuracy of modern global earthquake catalogs, Phys. Earth Planet Int., 135, 173–209, 2003.

Kagan, Y. Y.: On the geometric complexity of earthquake focal zone and fault systems: a statistical study, Phys. Earth Planet Int., 173, 254–268, 2009.

Kagan, Y. Y.: Earthquake size distribution: power-law with exponent $\beta = 1/2$?, Tectonophysics, 490, 103–114, doi:10.1016/j.tecto.2010.04.034, 2010a.

Kagan, Y. Y.: Statistical distributions of earthquake numbers: consequence of branching process, Geophys. J. Int., 180, 1313–1328, 2010b.

Kagan, Y. and Knopoff, L.: Earthquake risk prediction as a stochastic process, Phys. Earth Planet Int., 14, 97–108, 1977. 70, 71, 74, 75

Kagan, Y. and Knopoff, L.: Spatial distribution of earthquakes: the two-point correlation function, Geophys. J. R. Astro. Soc., 62, 303–320, 1980. 71
Kagan, Y. and Knopoff, L.: Stochastic synthesis of earthquake catalogues, J. Geophys. Res. 86, 2853–2862, doi:10.1029/JB086iB04p02853, 1981. 71
Kostrov, B. V.: Mechanics of Tectonic Earthquake Source, Nauka, Moscow, 173 pp., 1975. 74, 75
Kozlovskii, E. A. (Ed.): Mountain Encyclopedia, Vol. 1, Soviet Encyclopedia, Moscow, 560 pp., 1984. 81, 82
Lomize, M. G.: Volcanic ring of the Pacific Ocean, Sorosov Educ. J., 9, 59–66, 1999. 75, 82, 84
Lukk, A. A., Deshcherevskii, A. V., Sidorin, A. Y., and Sidorin, I. A.: Geophysical Field Variations as Deterministic Chaos Effect in Fractal Media, OIFZ RAS, Moscow, 210 pp., 1996. 70
Marapulets, Yu. V., Shevtsov, B. M., Larionov, I. A., Mishchenko, M. A., Shcherbina, A. O., and Solodchuk, A. A.: Geoacoustic emission response on deformation process activation during earthquake preparation, Pac. Geol., 31, 59–67, 2012. 84
Mardia, K. V.: Statistics of Directional Data, Academic Press Ltd, London, 357 pp., 1972. 77, 84
Metzler, R. and Klafter, J.: The random walk's guide to anomalous diffusion: a fractional dynamics approach, Reports, 339, 1–77, 2000. 72
Perezhogin, A. S., Shevtosv, B. M., Sagitova, R. N., and Vodinchar, G. M.: Simulation of geoacoustic zone emission, Math. Modelling, 19, 59–64, 2007. 73, 77
Rebetskii, Y. L.: Tectonic Stress and Natural Massif Strength, IKC "Akademkniga", Moscow, 406 pp., 2007. 75
Riznichenko, Y. V.: On Seismo-Tectonic Flow of Massifs, Earth Crust Dynamics, Nauka, Moscow, 56–63, 1965. 74, 75, 79, 82
Saichev, A. and Sornette, D.: "Universal" distribution of interearthquake times explained, Phys. Rev. Lett., 97, 078501, doi:10.1103/PhysRevLett.97.078501, 2006. 71
Saichev, A. I. and Zaslavsky, G. M.: Fractional kinetic equations: solutions and applications, Chaos, 7, 753–764, 1997. 71, 72
Shebalin, P. N.: Increased correlation range of seismicity before large events manifested by earthquake chains, Tectonophysics, 424, 335–349, 2006. 70, 71, 73, 74, 75, 80
Shevtsov, B. M. and Sagitova, R. N.: Statistical analysis of seismic processes on the basis of the deffusion approach, Dokl. Earth Sci., 426, 642–644, 2009. 70, 71, 72, 73, 74, 75

NPGD
2, 69–96, 2015

Non-local deformation effects in shear flows

A. V. Popova et al.

Shevtsov, B. M. and Sagitova, R. N.: Diffusion Approach in Statistic Analysis of Kamchatka Seismisity, No. 2, Volcanology and Seismology, Akademizdatcenter “Nauka” RAN, Moscow, 56–66, 2012. 70, 71, 72, 73, 74, 80

Sobolev, G. A. and Ponomarev, A. V.: Physics of Earthquakes and Harbingers, Nauka, Moscow, 270 pp., 2003. 70

Sornette, D. and Helmstetter, A.: Occurrence of finite-time singularities in epidemic models of rupture, earthquakes, and starquakes, Phys. Rev. Lett., 89, 158501, doi:10.1103/PhysRevLett.89.158501, 2002. 71

Vinogradov, S. D. and Ponomarev, V. S.: Experimental studying of a seismic mode, Priroda, 3, 77–89, 1999. 70

Zaliapin, I. and Ben-Zion, Y.: Earthquake clusters in southern California I: identification and stability, J. Geophys. Res.-Solid, 118, 2847–2864, 2013. 71

Zaliapin, I., Gabrielov, A., Keilis-Borok, V., and Wong, H.: Clustering analysis of seismicity and aftershock identification, Phys. Rev. Lett., 101, 018501, doi:10.1103/PhysRevLett.101.018501, 2008. 71, 72

NPGD

2, 69–96, 2015

Table 1. Clusters in the shear flow, constructed using the Dobrovolskiy model.

No. of clusters	No. of events in cluster	Date	Time	Magni-tude	Lat. (° S)	Long. (° E)	R_d (km)	R_t (days)	Δt (days)	ΔR (km)
23	23	21/11/1982	23:27:11	6.0	55.3	163.4	372.5	1074.8	757	1.04
	33	28/12/1984	10:37:53	6.5	56.2	163.8	647.2	3397.9	3040	7.02
	83	08/06/1993	13:03:37	7.4	51.4	158.8	1462.9	18579.9	1617	4.32
	136	05/12/1997	11:26:54	7.7	54.3	161.9	1969.6	34526.6	453	3.27
	172	08/03/1999	12:25:49	6.7	51.8	159.9	776.6	4966.8	930	1.09
	184	08/10/2001	18:14:26	6.3	52.6	160.6	492.9	1926.5	11×10^{-6}	0.54
	185	08/10/2001	18:20:38	6.1	53.1	160.9	439.9	1520.2	906	2.99
	209	14/04/2004	1:54:09	5.9	55.2	162.9	340.0	888.7	462	3.49
	219	26/07/2005	12:17:14	5.5	52.8	160.4	241.6	436.3	120	0.60
	221	26/11/2005	16:02:44	5.0	52.4	159.9	135.8	131.2		
47	47	06/10/1987	20:11:34	6.3	52.8	160.4	502.3	2003.6	1586	0.07
	70	02/03/1992	12:29:40	6.7	52.9	160.4	752.6	4652.0	456	2.19
	83	08/06/1993	13:03:37	7.4	51.4	158.8	1462.9	18579.9	1093	0.98
	110	21/06/1996	13:57:10	6.5	51.5	159.7	652.8	3458.8	700	1.55
	164	01/06/1998	5:34:03	6.3	52.9	160.4	490.3	1905.4	1141	4.87
	180	02/08/2001	23:41:06	6.1	56.3	163.9	424.3	1409.5	276	3.84
	192	08/05/2002	19:45:18	5.6	53.6	161.2	257.2	497.0	307	1.48
	195	15/03/2003	19:41:28	5.8	52.2	160.8	306.3	715.0	499	0.84
	212	04/08/2004	21:15:15	5.4	52.2	160.0	201.0	297.2	102	0.99
	213	16/11/2004	11:57:28	5.1	53.0	160.6	162.0	189.6	112	1.46
	214	08/03/2005	4:51:49	4.5	53.5	162.0	84.6	49.0		
62	62	19/12/1990	13:48:24	5.7	52.7	161.2	282.4	603.7	436	1.07
	71	05/03/1992	14:39:10	6.1	52.9	160.2	427.1	1429.5	457	2.70
	85	12/06/1993	20:33:26	6.0	51.0	158.2	386.0	1157.9	1090	1.53
	111	22/06/1996	14:50:07	5.9	51.3	159.7	357.7	987.9	523	3.30
	137	05/12/1997	18:48:22	6.2	53.7	162.0	480.4	1826.0	2	1.39
	147	07/12/1997	17:56:18	5.9	54.5	163.1	360.9	1006.2	170	3.87
	161	27/05/1998	20:41:37	5.7	52.2	160.0	292.0	647.3	281	0.41
	170	08/03/1999	5:40:00	5.5	52.1	159.6	234.8	410.9	32×10^{-6}	0.43
	171	08/03/1999	5:57:52	5.5	52.0	160.0	231.4	398.7	245	0.21
	174	13/11/1999	21:24:46	5.1	51.9	160.2	148.6	158.4		

NPGD
2, 69–96, 2015

Title Page
Abstract | Introduction
Conclusions | References
Tables | Figures
◀| |▶
◀ ▶
Back | Close
Full Screen / Esc
Printer-friendly Version
Interactive Discussion

Table 1. Continued.

No. of clusters	No. of events in cluster	Date	Time	Magni-tude	Lat. (° S)	Long. (° E)	R_d (km)	R_t (days)	Δt (days)	ΔR (km)
77	77	13/07/1992	15:34:05	5.9	50.8	158.2	352.8	960.1	156	1.36
	81	19/12/1992	12:14:22	5.8	52.0	158.9	309.1	728.6	328	0.43
	89	17/11/1993	11:18:52	5.8	51.7	159.3	300.7	687.9	494	0.50
	98	01/04/1995	5:50:20	5.7	52.0	159.7	292.0	647.3	449	0.70
	120	30/06/1996	11:32:35	5.8	51.7	160.3	318.7	776.5	516	2.94
	144	06/12/1997	10:59:10	5.9	53.9	162.3	327.8	823.5	23×10^{-5}	0.99
	145	06/12/1997	12:37:21	5.7	54.8	162.6	275.4	572.8	1	1.18
	148	07/12/1997	23:05:50	5.3	53.7	162.2	199.4	292.2	263	0.21
	167	30/08/1998	14:34:43	5.3	53.6	162.3	185.5	251.6	144	0.94
	169	24/01/1999	13:15:52	5.1	54.3	161.7	161.6	188.7		
90	90	07/01/1994	3:42:42	5.4	51.7	159.6	213.4	336.6	37	43.75
	91	14/02/1994	11:14:25	5.6	51.7	159.5	257.1	496.5	83	31.12
	94	07/05/1994	8:31:36	5.5	52.7	160.6	226.0	379.6	331	43.85
	99	08/04/1995	19:13:51	5.3	52.2	159.1	182.2	242.2	224	45.11
	101	22/11/1995	20:56:04	5.0	52.1	159.5	137.1	133.9	79	1.34
	107	11/02/1996	23:51:01	5.0	51.8	160.9	137.3	134.3	132	123.62
	115	23/06/1996	12:45:06	5.6	51.5	159.7	260.9	511.8	25	17.61
	122	18/07/1996	22:55:03	5.5	51.4	159.8	243.3	442.4	74	84.27
	126	02/10/1996	16:00:20	5.1	53.2	160.7	159.0	182.4	179	20.39
	129	31/03/1997	19:36:06	5.0	53.2	161.9	138.6	137.1		
131	131	16/05/1997	22:41:03	5.2	55.6	163.1	173.4	218.6	200	1.48
	142	06/12/1997	6:38:00	5.3	54.5	162.1	193.8	275.5	46×10^{-5}	0.92
	143	06/12/1997	10:05:04	5.4	53.6	162.4	210.6	327.6	2	0.23
	150	08/12/1997	21:06:13	5.3	53.7	162.1	183.9	247.0	2	1.50
	153	10/12/1997	8:08:17	5.1	54.8	163.1	159.8	184.2	1	0.42
	154	11/12/1997	4:00:32	4.9	55.0	163.5	123.9	108.4	4	0.46
	156	15/12/1997	22:58:42	4.8	55.3	163.7	121.1	103.4		

NPGD
2, 69–96, 2015
Non-local deformation effects in shear flows
A. V. Popova et al.

Table 2. Clusters in the shear flow, constructed using the Mindlin model.

No. of clusters	No. of events in cluster	Date	Time	Magni-tude	Lat. (° S)	Long. (° E)	R_d (km)	R_t (days)	Δt (days)	ΔR (km)
	8	23/01/1980	1:51:44	5.6	52.2	160.7	43.5	517.1	11×10^{-5}	0.10
	9	23/01/1980	2:34:12	5.4	52.3	160.8	68.5	358.2	68×10^{-5}	0.14
8	11	23/01/1980	8:12:26	5.3	52.2	160.7	46.8	286.7	2	0.28
	13	25/01/1980	11:38:55	5.2	52.0	160.8	70.8	203.2		
	46	06/10/1987	20:11:34	6.3	52.8	160.4	71.1	2003.6	1586	0.07
	69	02/03/1992	12:29:40	6.7	52.9	160.4	67.6	4652.0	3456	0.33
	141	08/10/2001	18:14:26	6.3	52.6	160.6	71.6	1926.5	11×10^{-6}	0.54
46	142	08/10/2001	18:20:38	6.1	53.1	160.9	59.2	1520.2	1368	0.50
	166	26/07/2005	12:17:14	5.5	52.8	160.4	54.6	436.3	120	0.60
	167	26/11/2005	16:02:44	5.0	52.4	159.9	62.8	131.2		
	88	01/04/1995	5:50:20	5.7	52.0	159.7	59.8	647.3	442	0.49
	98	23/06/1996	12:45:06	5.6	51.5	159.7	58.7	511.8	7	0.65
	103	30/06/1996	11:32:35	5.8	51.7	160.3	61.0	776.5	18	0.53
88	105	18/07/1996	22:55:03	5.5	51.4	159.8	69.1	442.4	290	0.20
	109	08/05/1997	6:07:09	5.1	51.5	159.7	72.9	181.4	41	0.39
	110	19/06/1997	22:45:32	4.8	51.3	160.0	80.8	97.8		
	94	22/06/1996	14:50:07	5.9	51.3	159.7	39.6	987.9	1	0.29
	95	23/06/1996	1:17:56	5.2	51.5	159.8	42.6	215.7	15×10^{-4}	0.33
94	99	23/06/1996	14:58:30	5.1	51.5	159.4	67.6	167.5	68×10^{-5}	0.82
	100	23/06/1996	20:19:28	4.9	51.2	160.2	78.8	121.7		
	111	05/12/1997	18:48:22	6.2	53.7	162.0	61.0	1826.0	1	0.37
	114	06/12/1997	10:59:10	5.9	53.9	162.3	53.7	823.5	1	0.21
111	115	07/12/1997	23:05:50	5.3	53.7	162.2	38.5	292.2	263	0.21
	128	30/08/1998	14:34:43	5.3	53.6	162.3	60.1	251.6		
	112	06/12/1997	0:25:06	5.5	53.7	161.8	60.9	394.1	10×10^{-4}	0.61
	113	06/12/1997	10:05:04	5.4	53.6	162.4	60.8	327.6	2	0.23
112	117	08/12/1997	21:06:13	5.3	53.7	162.1	50.3	247.0	11×10^{-5}	0.08
	118	08/12/1997	22:19:55	5.1	53.6	162.2	45.6	168.6	18	0.19
	121	26/12/1997	5:02:32	5.0	53.4	162.2	60.8	130.4		
	124	27/05/1998	20:41:37	5.7	52.2	160.0	63.4	647.3	281	0.41
	130	08/03/1999	5:40:00	5.5	52.1	159.6	48.5	410.9	32×10^{-6}	0.43
124	131	08/03/1999	5:57:52	5.5	52.0	160.0	58.5	398.7	245	0.21
	134	13/11/1999	21:24:46	5.1	51.9	160.2	69.5	158.4		

NPGD
2, 69–96, 2015

Non-local deformation effects in shear flows

A. V. Popova et al.

Table 3. Shear flow characteristics where the Dobrovolskiy spatial radius is used.

No.	k	τ, (days)	Energy, (J) $\overline{E}$	ΣE	$\overline{u}$, (sm)	γ	MAD	$\overline{v}$, (sm year^{-1})	ξ, (year^{-1})
23	10	8405	2.2×10^{15}	2.2×10^{16}	35	311.7°	18.6°	15	2.1×10^{-6}
47	11	6362	7.7×10^{14}	8.5×10^{15}	26	307.2°	9.8°	17	2.4×10^{-6}
62	10	3251	4.8×10^{13}	4.8×10^{14}	17	302.6°	10.9°	19	3.3×10^{-6}
77	10	2385	2.4×10^{13}	2.4×10^{14}	14	299.3°	12.9°	21	3.4×10^{-6}
90	10	1179	7.8×10^{12}	7.8×10^{13}	10	307.5°	9.2°	30	5.9×10^{-6}
131	7	213	4.1×10^{12}	2.9×10^{13}	8	312.1°	12.6°	98	3.4×10^{-5}

NPGD
2, 69–96, 2015

NPGD
2, 69–96, 2015

Non-local deformation effects in shear flows

A. V. Popova et al.

Table 4. Shear flow characteristics where the spatial radius calculated in the Mindlin model is used.

No.	k	τ (days)	Energy (J), $\overline{E}$	ΣE	$\overline{u}$ (sm),	γ	MAD	$\overline{v}$ (sm year^{-1})	ξ (year^{-1})
8	4	2	9.2×10^{12}	3.7×10^{13}	11	229.2°	4.8°	7745	4.4×10^{-3}
46	6	6625	1.9×10^{14}	1.1×10^{15}	23	227.7°	10.5°	8	9.5×10^{-8}
88	6	810	1.6×10^{13}	9.4×10^{13}	12	311°	12.3°	32	9.9×10^{-6}
94	4	1	1.5×10^{13}	5.9×10^{13}	10	303.4°	10.7°	14932	6.8×10^{-3}
111	4	267	4.8×10^{13}	1.9×10^{14}	15	244.8°	12°	85	3.0×10^{-5}
112	5	20	5.7×10^{12}	2.8×10^{13}	9	298.6°	10.8°	825	4.0×10^{-4}
124	4	535	1.3×10^{13}	5.0×10^{13}	11	235.9°	12.3°	31	6.6×10^{-6}

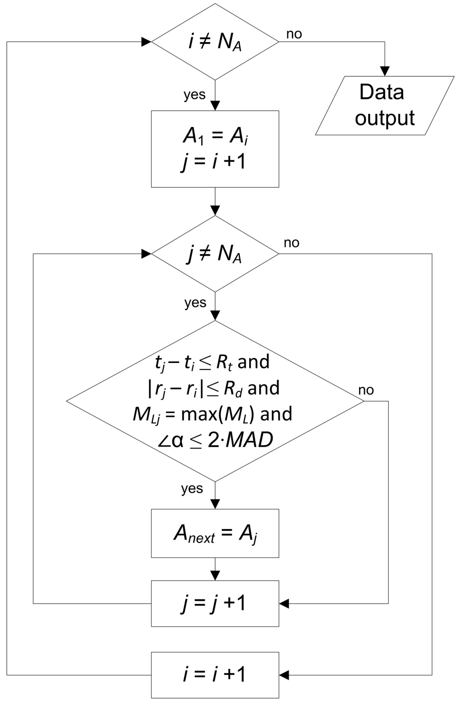

Figure 1. The block diagram of the algorithm of creation of clusters. Legend: i, j – number of events in the sample; A – event in the sample; N_A – the total number of events in the sample; $(t_j - t_i)$ – time period between events A_j and A_i; $|r_j - r_i|$ – the distance between the hypocentres of events A_j and A_i; M_{Lj} – Richter magnitude for event A_j; α – angle between the direction of displacement of events A_j and A_i; A_1 – first event of the cluster; A_{next} – next connected event of the cluster.

NPGD
2, 69–96, 2015

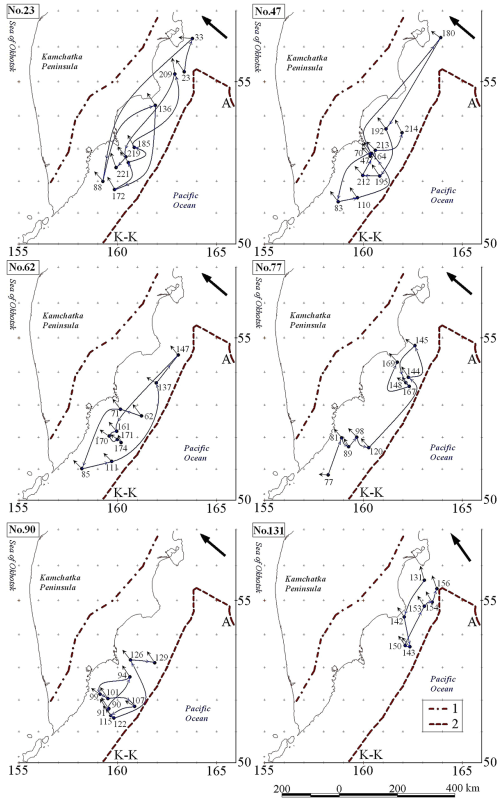

Figure 2. The largest clusters in the shear flow, where the spatial radius of influence was calculated by the Dobrovolskiy model. Notations: 1 – schematic view of the largest faults; 2 – axis of deep trenches: Kuril–Kamchatka (K–K) and Aleut (A). Arrows indicate the projections of dislocation shift directions, and the bold arrow indicates the projection of the main flow direction in the cluster. Connected events are connected sequentially by blue arrows.

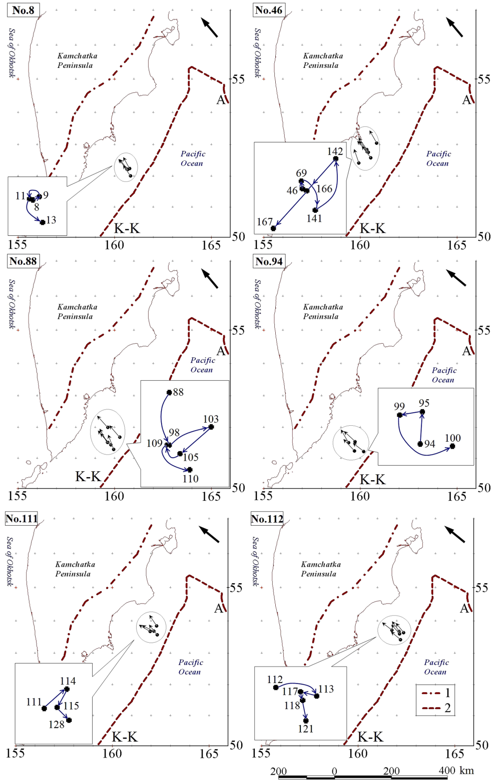

Figure 3. The largest clusters in the shear flow, where the spatial radius of influence was calculated by the Mindlin model. Notations: 1 – schematic view of the largest faults; 2 – axis of deep trenches: Kuril–Kamchatka (K–K) and Aleut (A). Arrows indicate the projections of dislocation shift directions, and the bold arrow indicates the projection of the main flow direction in the cluster. Connected events are connected sequentially by blue arrows.